

A new design and manufacturing process for embedded Lamb waves interdigital transducers based on piezopolymer film

Filippo Bellan^a, Andrea Bulletti^{a,*}, Lorenzo Capineri^a, Leonardo Masotti^a,
Goksen G. Yaralioglu^b, F. Levent Degertekin^c, B.T. Khuri-Yakub^b,
Francesco Guasti^d, Edgardo Rosi^d

^a Department of Electronics and Telecommunications, Ultrasound and Non-Destructive Testing Laboratory, University of Florence,
Via S. Marta 3, 50139 Florence, Italy

^b E.L. Ginzton Laboratory, room 11, Stanford University Stanford, CA 94305-4088, USA

^c G.W. Woodruff School of Mechanical Engineering, Georgia Institute of Technology, 801 Ferst Dr. NW,
Atlanta, GA 30332-0405, USA

^d Alenia Spazio – Laben, Proel Technologie plant, Einstein 35, 50013 Campi Bisenzio, Florence, Italy

Received 1 October 2004; received in revised form 18 April 2005; accepted 20 May 2005

Available online 29 June 2005

Abstract

In this work a new technology for designing and manufacturing ultrasonic interdigital transducers (IDT) is presented. The piezoelectric material used is a metallised piezopolymer film made of polyvinylidene fluoride (PVDF) with electrode pattern obtained with a laser ablation process. Piezopolymer transducer prototypes are designed with wavelength of 8 mm to operate with Lamb waves (symmetrical S_0 mode). An experimental validation of the piezopolymer IDT design is demonstrated with a transmitter-receiver IDT pair embedded in a 3 mm thick carbon fiber reinforced plastic (CFRP) composite laminate.

Acoustical response and the electrical impedance have been calculated.

These transducers are proposed for monitoring structural integrity of structures/components made of carbon epoxy composite laminates commonly used in spacecrafts, satellite and airplanes.

© 2005 Elsevier B.V. All rights reserved.

Keywords: Interdigital transducers; Polyvinylidene fluoride (PVDF); Lamb waves; Carbon fiber composites; Smart materials; Non-destructive testing (NDT)

1. Introduction

Lamb wave transducers are widely used for monitoring the health of structures made of laminated materials (metals, composites) [1]. These piezoelectric ultrasonic transducers transmit/receive acoustic guided waves that interact with the elastic properties of the material under investigation. In many non-destructive testing (NDT) systems, acoustic guided waves are generated and detected by piezoelectric transducers that are acoustically coupled with the laminate sample. Assuming a comparable thickness, d of the laminates

with the wavelength, λ , the ultrasonic propagation of guided waves is dispersive and it is governed by the Rayleigh–Lamb wave equations [2]. A variation of the acoustoelastic properties of the composite material, for example, due to a damage caused by an overstress or impact, changes the propagation characteristics of an ultrasonic signal and suitable signal processing can reveal defects (delaminations, debonding, inclusions, cracks) non-destructively. An important application of this NDT method is for monitoring of large structures made of composite materials and it has been also the objective of a research activity carried out by some of the authors [3]. In this previous work, it has been developed a new design and manufacturing process for interdigital transducers (IDTs) with a polyvinylidene fluoride (PVDF) piezopolymer film.

* Corresponding author. Tel.: +39 055 4796383; fax: +39 055 4796517.
E-mail address: bulletti@det.unifi.it (A. Bulletti).

This piezoelectric material has been already used to fabricate ultrasonic transducers for NDT applications and some related works can be found in [4–6].

In this work, the interdigital transducer configuration has been adopted to ensure a more strict control on the excitation/detection of the selected acoustic wave guided modes instead of a single element broadband transducer. It is well known that PVDF has some features not found in piezoceramics: lightweight, low cost, non-fragility and conformable to the surface of materials. Bearing in mind these characteristics, we believe PVDF suited for devising transducers to be employed for monitoring of composites. In particular its conformability is very important to make easy and efficient acoustic coupling of the IDT with curved surfaces, typical of space components such as pipes, pressure vessels, tanks, etc. On the contrary a limited temperature range (-40°C , $+110^{\circ}\text{C}$) and lower electromechanical coupling factor ($K_{\text{T(PVDF)}} = 0.11\text{--}0.14$) than PZT ($K_{\text{T(PZT)}} = 0.4\text{--}0.5$) counterbalance these unique features. Extended temperature limits (up to 110°C) can be obtained by using a copolymer (P(VDF-TrFE)) instead of PVDF.

In Section 2, the design of IDT electrode pattern dimensions according to the estimated dispersion curves of the target CFRP composite laminate is presented. In Section 3, the manufacturing technology is described. The validation of this ultrasonic transducer technology was already tackled in the previous research work [3], where the IDTs were bonded on one side of different types of CFRP laminates and tested for the detection of artificial defects. A new development of this research is the study of PVDF IDTs embedded in a CFRP laminate. The advantages of embedding the transducer in the composite structure are the improved acoustic coupling and the protection of transducer from external environment (accidental impacts, dust, scratches, etc.). In this work the IDT transducer has been inserted in the middle of two unidirectional (UD) CFRP composite laminates (each one 1.5 mm thick) that are bonded together with epoxy glue.

The acoustic response and the electrical impedance of the fabricated transducers are calculated in Section 4 and the results of the experimental characterisation with symmetrical S_0 guided mode are illustrated in Section 5. Finally, a comparison between the experimentally observed symmetrical propagation modes and those expected from the numerical evaluation are reported.

2. Definition of the interdigital transducer geometry by simulations

The first objective of the design of an IDT is the definition of the electrode pattern, which under certain hypothesis defines the frequency response, and the selection of a propagation mode according to the laminate dispersion curves [4,7]. The first assumption in our design is that the PVDF thickness can be neglected respect to the thickness of CFRP (in our sample PVDF thickness is $100\ \mu\text{m}$ and CFRP sample

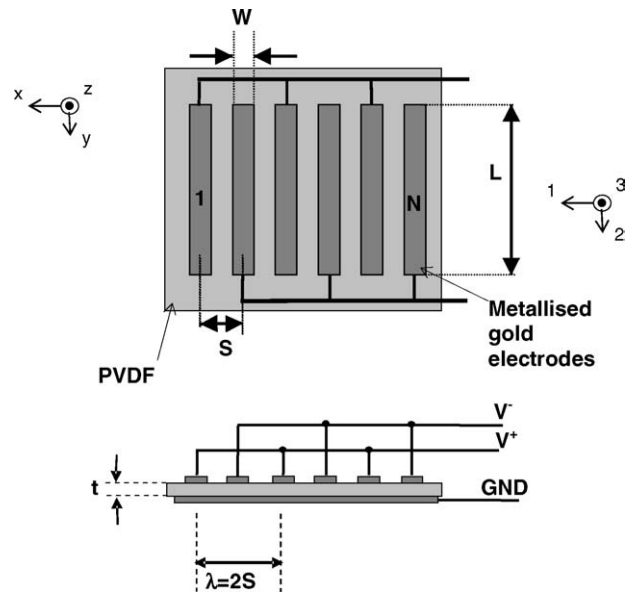


Fig. 1. Configuration of an IDT bonded on a laminate. (Top) plane view, (bottom) cross-section view. Drawing not in scale.

thickness is 3 mm). This condition has an important consequence in transducer design, because in this way the wave guide for the Lamb wave is only the CFRP sample, and then has been possible to use the dispersion curves of CFRP directly.

The IDT electrode geometry is shown in Fig. 1, where the interlaced electrode configuration has been adopted. This transducer configuration is differential, because the two series of electrodes (also called fingers) are driven with opposite phase signals (V^+ and V^-) and they have the same reference ground electrode (GND). The basic transducer design parameters are: width (W); length (L); piezopolymer film thickness (t); fingers separation (S); and number of fingers (N). The interlaced configuration requires that finger separation, S , must be half of the wavelength, λ relative to the selected guided wave mode.

The parameter, W changes the effective area of IDT and also influences the acoustic response in wavenumber $k = 2\pi/\lambda$ domain. The length, L defines the directivity of the transducers according to the approximated relationship for laminates [8]:

$$\gamma = \sin^{-1} \left(\frac{\lambda}{L} \right) \quad (1)$$

where γ is the beam divergence angle.

The propagation mode selection on the CFRP dispersion curves (phase velocity V_P versus frequency-laminate thickness product $f \times d$) can be predicted by the following relationship between λ , d , and V_P :

$$\frac{V_P(fd)}{f_0 d} = \frac{\lambda}{d} \quad (2)$$

where f_0 is the transducer operating frequency.

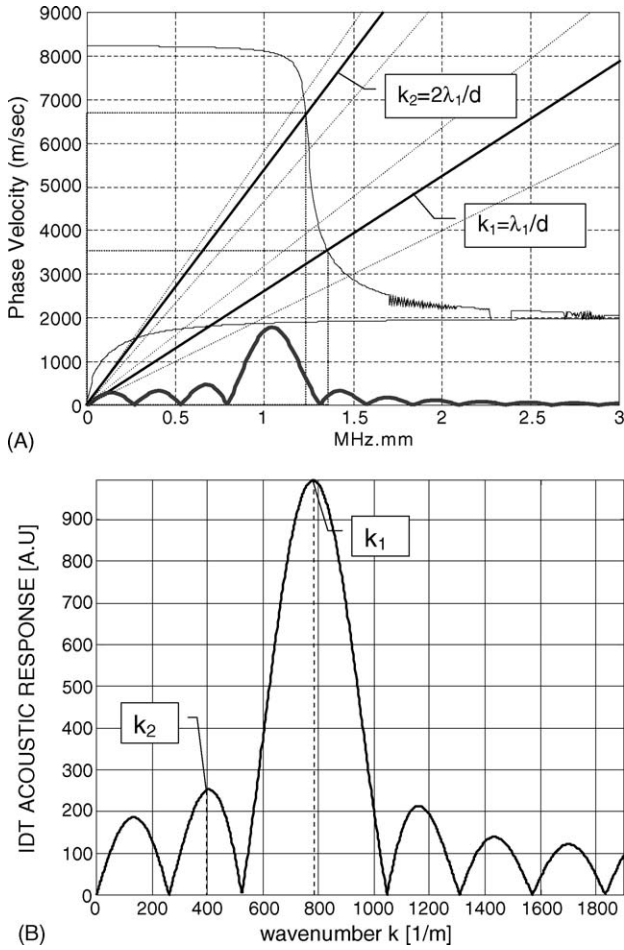


Fig. 2. (A) Dispersion curves for A0 and S0 for CFRP. The propagation directions are reported in the reference system in Fig. 1. The material properties used in the calculations are: for CFRP, $C_{11} = 9.6 \times 10^9$; $C_{23} = 4.48 \times 10^9$; $C_{33} = 103 \times 10^9$; $C_{55} = 6.24 \times 10^9$; $C_{66} = 3.7 \times 10^9$ Pa; density = 1490 kg/m^3 ; for PVDF (assumed isotropic with $V_{\text{long}} = 2200 \text{ m/s}$ and $V_{\text{shear}} = 1500 \text{ m/s}$) $C_{11} = 8.6 \times 10^9$; $C_{44} = 4 \times 10^9$ Pa. Density = 1780 kg/m^3 . (B) Acoustic response of the interdigital transducer in the wavenumber domain according to the electrode geometry. For convenience of the guided mode analysis the same response is reported at the bottom of Fig. 2A in the $f \times d$ domain.

The intersections between the straight line (λ/d) and the dispersion curves define all the possible excitation modes for an IDT coupled to a specified laminate. These modes are identified by specific values of $f \times d$.

In order to calculate the dispersion curves of the manufactured UD CFRP we measured the elastic constants. We found values close (within 9%) with those of another similar composite reported in the literature [9]. Fig. 2A reports the simulated curves for A_0 and S_0 phase velocity [10] for our laminate calculated in the interval of $f \times d$ (0–3 MHz mm).

Dispersion curves were calculated using the surface impedance method. The phase velocity of the propagating modes was found by searching the zeros of the determinant of the surface impedance tensor [11]. The sudden jumps on the A_0 and S_0 phase velocity above 1.5 MHz mm is due to the existence of other propagating modes. While the search algorithm was forced to track the velocity of the certain modes, it sometimes also tracked the velocities of the other modes when the phase velocities were close to each other as shown in Fig. 2A.

From these curves we observed that the S_0 mode started with a velocity of about 8200 m/s and had a low dispersion until an $f \times d$ of about 1 MHz mm. Both S_0 and A_0 tend to a Rayleigh velocity of about 2000 m/s.

In our previous IDT design for another composite type [3] we developed an IDT with finger separation $S = \lambda_1/2 = 3.95 \text{ mm}$, number of finger pairs $N_{\text{FP}} = N/2 = 3$ and a finger width $W = 1.7 \text{ mm}$.

Assuming that the frequency response of the IDT is the Fourier transform of its charge spatial distribution [7], defined by the electrode geometry, we calculated the transducer response in the wave number domain, k . Fig. 2B reports the simulated acoustic response in the wave number domain k ; we can individuate a first main peak at $k_1 = 795 \text{ m}^{-1}$ (or $\lambda_1 = 2S = 7.9 \text{ mm}$) that arise from the synchronous contribution of the three fingers pairs. A second lobe with a relative maximum at $k_2 = k_1/2 = 397 \text{ m}^{-1}$ formed by the contribution of the two finger pairs with same phase at distance $\lambda_2 = 2\lambda_1 = 15.8 \text{ mm}$ (see Fig. 1). The plotting of the corresponding straight lines (λ/d) defined by the values of λ_1 and λ_2 on the dispersion curves of Fig. 2A, defines the selection of symmetrical propagation modes in the composite laminate with thickness $d = 3 \text{ mm}$. Table 1 contains numerical values estimated for these two IDT operating points on the S_0 curve.

The interpretation of these values leads to the consideration that it is possible to use this IDT geometry to demonstrate the embedded transducer application, by exciting the IDT with a signal spectrum covering the bandwidth from 414 to 452 kHz. A tolerance is also expected due to the finite width of fingers W , which enlarge the range of possible intersections around each straight line on the S_0 . This effect is shown in Fig. 2A by the thin lines embracing the two thick lines corresponding to k_1 and k_2 . As we will show later in the experimental section, we have enough sensitivity for this IDT to measure these two propagation modes along a distance of about 50 cm. If the design goal is to work in the region of S_0 mode with low dispersion, is sufficient to redesign a new IDT with larger finger separation (i.e. $3\lambda_1$), while a higher selectivity is obtained by increasing the number of finger pairs N_{FP} . Both modifications lead to an IDT with larger surface; consequently the increased capacitance influences the reso-

Table 1
Numerical values estimated for two IDT operating points on the S_0 curve

$k_1 = 2\pi/\lambda_1$	$\lambda_1/d = 2.63$	$V_{S_0'} = 3573 \text{ m/s}$	$f_0' = 452 \text{ kHz}$	$f_0' \times d = 1.35 \text{ MHz mm}$
$k_2 = 2\pi/\lambda_2$	$\lambda_2/d = 5.26$	$V_{S_0''} = 6750 \text{ m/s}$	$f_0'' = 414 \text{ kHz}$	$f_0'' \times d = 1.24 \text{ MHz mm}$

nant characteristic and the electronic front-end but there are not added difficulties for the manufacturing process as will be shown in the next section. From the above considerations, the IDT can be easily designed with a geometry that is versatile for using the same transducers for testing different types of composites with Lamb waves, as already pointed out in the paper of Veidt et al. [12].

Finally, according to Eq. (1), the calculated beam divergence γ is 33.6° assuming $L = 14.45$ mm; this value of beam divergence means that enough signal intensity can be picked-up at distances around 50 cm and the influence of reflected signals from the composite edges are negligible.

3. Interdigital transducer manufacturing technology

The material used for the sensor design is a commercial copolymer P(VDF-TrFE) film (PiezoTech s.a., St. Louis, France) with thickness $t = 100$ μm and a gold metallisation with approximate thickness of 0.1 μm , mass density $\rho_m = 1780$ kg/m, and longitudinal velocity $V_L = 2200$ m/s. Other material properties are reported in Table 2.

There are some general considerations useful to justify the choice of this piezoelectric material for embedded transducers:

- (1) The material is a dielectric and when it is metallised on both surfaces for making electrodes, it acts substantially as a capacitor outside of the resonance frequency.
- (2) The acoustic impedance is $Z_{\text{PVDF}} = \rho_m V_L = 4.18$ MRayl that is not so far from a typical acoustic impedance of

our composite material that is in the order of 3.78. This means a good acoustic matching and an easier acoustic energy transfer.

- (3) Z_{PVDF} changes up to 30% in temperature range -40°C to 110°C according to the dependence of the PVDF longitudinal velocity from temperature.
- (4) The typical electromechanical coupling factor $k_T = 0.14$ is about four times lower than that of the piezoceramic materials [13].
- (5) The mechanical flexibility of this special “plastic” material is certainly an advantage for space applications where mechanical vibrations or stress can be envisaged.

Moreover, with suitable composite fabrication processes, the PVDF material can also be embedded in the composite structure leading to a real smart material with self-diagnostic capabilities. On the contrary piezoceramic materials are fragile and subjected to microfractures when mechanically shocked.

For electrode design on the PVDF film we have used a fast manufacturing process based on laser ablation of the thin film metallization on both film surfaces that is now common in many electronic production processes [14]. This process has been developed for pyroelectric arrays and it is based on the migration of the CAD drawing on the PVDF film by a Nd:YAG laser marking tool [15,16]. This file is directly transferred to the laser equipment (LASIT, El.En. SpA, Italy) and the processing time for each transducer is about 1 min. By tuning the laser marking system parameters specifically for the target film, it is possible to avoid mechanical damage due to overheating. This laser micromachining process is simple, low cost and reproducible for patterning electrodes of arbitrary geometry and becomes competitive with other well-known methods like etching or screen printing of conductive ink [17]. Another advantage of this solution is the possibility to depolarize the piezopolymer film during the laser ablation process of the film metallization. Once this condition is achieved the PVDF material between fingers is depolarized and then becomes partially inactive, decreasing the cross-coupling between fingers.

In Fig. 3 is shown one IDT prototype bonded on the surface of a unidirectional composite laminate.

4. Simulations of the IDT acoustic response and electrical impedance

The final step of the IDT design is the simulation of the acoustic response and electrical impedance. By these simulations we can analyse the piezoelectric behaviour of the piezopolymer IDT in the frequency domain and we can verify if at the desired operating frequency we have an efficient excitation of the Lamb wave. Moreover, the evaluation of the electrical impedance is necessary to design a custom electronics: a linear amplifier driver for the Tx-IDT and an instrumentation amplifier for Rx-IDT [3]. The simulations

Table 2
Materials properties

Parameter	Symbol	Value
PVDF		
Thickness	t	100 μm
Electromechanical coupling factor (at 1 kHz)	k_T	0.14
Electrical loss tangent (at 1 kHz)	$\tan(\delta_e)$	0.015
Mechanical loss tangent (at 1 kHz)	$\tan(\delta_m)$	0.1
Mass density	ρ_m	1900 kg/m ³
Longitudinal velocity	V_L	2200 m/s
Acoustic impedance	Z_{CFRP}	4.18×10^6 kg/(m ² s)
CFRP		
Acoustic impedance	Z_{CFRP}	3.78×10^6 kg/(m ² s)
Mass density	ρ_{CFRP}	1490 kg/m ³
Stiffened elastic constant	C_{11}	9.6×10^9 N/m ²
Single laminate thickness	$d/2$	1.5 mm
Epoxy		
Acoustic impedance	Z_{epoxy}	2.68×10^6 kg/(m ² s)
Mass density	ρ_{epoxy}	1100 kg/m ³
Stiffened elastic constant	C_{epoxy}	6.54×10^9 N/m ²
Thickness	d_{epoxy}	0.1 mm
Air		
Air acoustic impedance	Z_{AIR}	444 kg/(m ² s)

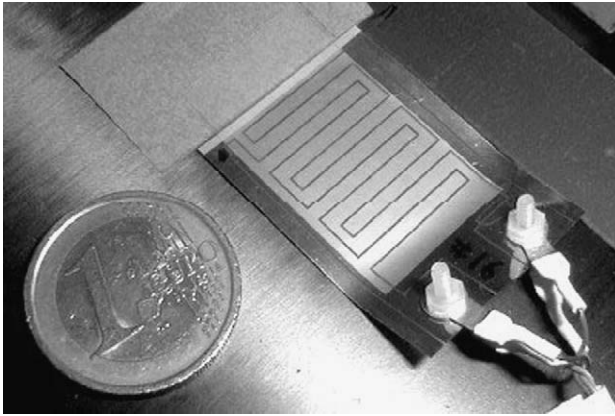


Fig. 3. Prototype of the interdigital piezopolymer transducer bonded on a unidirectional 1.5 mm thick unidirectional CFRP laminate before the application of the epoxy.

are referred to an embedded IDT in a composite, made of two unidirectional CFRP laminates ($d/2 = 1.5$ mm thick each) bonded together with epoxy glue of about 0.1 mm thickness.

The Tx and Rx IDTs are inserted in the middle of the two composites and electrically isolated with a thin Teflon film. As a first approximation, the thickness of the gold metallisations and the Teflon film were neglected with respect to the PVDF and CFRP thickness. In Fig. 4 the schematic drawing of a section in x - z plane of the embedded IDT validation model is shown. The guided wave generated by the Tx-IDT travels along the direct path to the Rx-IDT placed at a distance $D = 437$ mm. Electrical contacts to IDTs are made by means of three wires cables coming out from the two composite edges.

The electrical input impedance (Z_{IN}) is measured between V^+ (or V^-) and GND and considers N_{FP} fingers in parallel; the input current at the transducer electrical port is called I_3 . The force applied to the composite by a single finger due to the inverse piezoelectric effect is called F_2 and it has the same modulus for positive and negative phase fingers. The latter assumption is due to the symmetric voltage excitation V^+ and V^- and the symmetry of the CFRP model shown in Fig. 4. The acoustic response is defined by the ratio F_2/I_3 .

There are several transducer models that can be used to determine the electrical input impedance and acoustic

response of an interdigital transducer. For surface acoustic wave (SAW) transducers, the normal-mode theory, which is based on the conservation of power, has been applied and described in [7]. For the study of Lamb wave modes propagation in IDT applications to CFRP, Veidt et al. [12] has developed an equivalent model for the Lamb wave propagation based on the discrete layers and multiple integral transform and the outputs are time domain signals and wavenumber spectrum. More recently, another method has been presented by Jin et al. [18]. The latter two models are very powerful but don't consider the piezoelectric transducer design. In this work the piezoelectric characteristics of the manufactured piezopolymer IDTs have been simulated with a simplified approach, described below.

Our approach is based on the well-known equivalent-circuit method (three-port model) described in [7] and [19], valid for a single piezoelectric element. In the case of our IDT this model has been modified for considering a series of fingers in parallel. An analysis of the applicability of this model according to actual IDT dimensions has been performed and then validated with experimental measurements described in the next section. In the three-port model, shown in Fig. 5, we have an electrical input port which defines $Z_{IN} = V_3/I_3$ and two acoustic ports which define the acoustic loads on both surfaces of a single finger. Due to the symmetry of the designed CFRP model the two acoustic ports (port 1 and 2) have the same acoustic load, schematically represented with the blocks A_{epoxy} and A_{CFRP} . In fact the epoxy glue and CFRP layers are present on both sides of the PVDF transducer.

Considering the cross-section view of the IDT shown on the bottom of Fig. 1, we can evaluate the electric field distribution due to the application of a voltage V^+ (or V^-) to the N_{FP} electrodes connected in parallel. This analysis is important because we need to assume only a vertical electrical field (E_z) for the application of the three-port model. In an IDT there is also a horizontal (E_x) component of the electric field, which influences the piezoelectric response of an IDT. In [7] these two conditions are referred to the "in-line model" (only E_x) and the "crossed-field model" (only E_z) for an IDT and they are used together to represent the actual spatial distribution of the real electric field.

We now evaluate numerically E_x and E_z , considering the electrical field equation of two infinite parallel planes, one along x and the other along z a good approximation of our

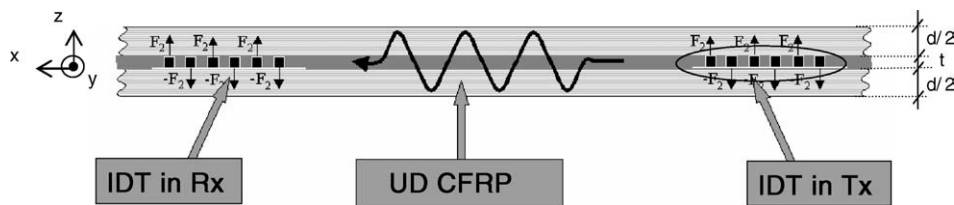


Fig. 4. Schematic drawing of an IDT pairs embedded in a unidirectional CFRP sample. The reference axis of the experiment is shown and the the polarization axis '1', '2', '3' of the piezo-polymer film.

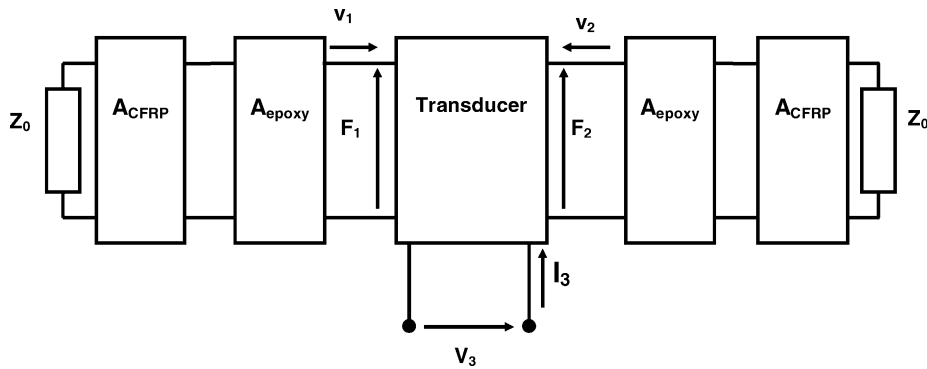


Fig. 5. Equivalent three-port model for piezoelectric interdigital transducer. Parameters description for layers 1 and 2: F_i : force (N) $i=1, 2$; v_i : longitudinal velocity (m/s) $i=1, 2$; V_3 : voltage (V); I_3 : current (A); A_{epoxy} : acoustic transmission line matrix of the epoxy glue layer; A_{CFRP} : acoustic transmission line matrix of the unidirectional CFRP layer; Z_0 : characteristic impedance of the semi-infinite medium (air in our case).

case:

$$E_x = \frac{|V^+ - V^-|}{S - W} = 2 \frac{|V^+|}{S - W} = 0.89 |V^+| \tag{3}$$

$$E_z = \frac{|V^+|}{t} = 10 |V^+|$$

where $|V^+| = |V^-|$ is assumed for a differential voltage excitation/detection and assuming the dimensions of S , W and t in mm.

From (3) we can calculate the ratio $E_z/E_x = 11.2$. This means that the total electric field is almost perpendicular to the direction x of the propagation of the Lamb wave, as illustrated in Fig. 4.

According to this result we have implemented the three-port model with a Matlab® program, which carries out the numerical calculations of Z_{IN} and the acoustic response F_2/I_3 . In Table 2 are reported the simulation input parameters for the PVDF transducer and the epoxy glue and unidirectional CFRP layers.

The simulated acoustic response, shown in Fig. 6, exhibits a first resonance at 313 kHz (f_{R1}) and a second harmonic resonance at 630 kHz (f_{R2}).

In Fig. 7 is shown the simulation results of the IDT electrical impedance Z_{IN} over the same frequency range of Fig. 6. The plot of the electrical impedance have two weak resonances at frequencies f_{R1} and f_{R2} . The weak resonance behaviour was expected due to the piezoelectric characteristics of the PVDF material, especially when compared with PZT. The mechanical load on both sides of the PVDF film has also the effect of shifting the resonance to lower frequency.

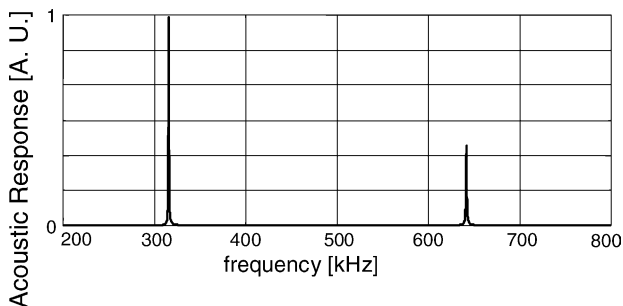


Fig. 6. Simulated acoustic response of interdigital transducer.

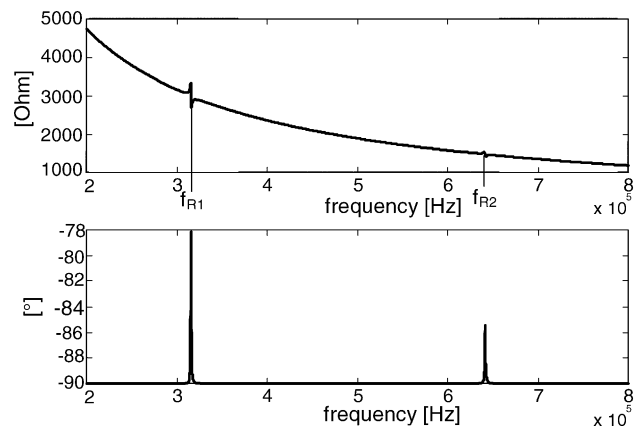


Fig. 7. Simulated electrical impedance Z_{IN} of the embedded interdigital transducer: magnitude (top) and phase (bottom).

teristics of the PVDF material, especially when compared with PZT. The mechanical load on both sides of the PVDF film has also the effect of shifting the resonance to lower frequency.

5. Experimental results

The experimental part of this work is aimed to validate the IDT design and simulation processes described above. The experimental set up with electronic instruments and the composite sample with a pair of embedded IDT is illustrated in Fig. 8.

In order to check the efficiency of the embedded IDTs when operated around the first or the second resonance frequency, we measured the magnitude and phase of input impedance (see Fig. 9). We found very weak resonances as expected for the PVDF material as shown in Fig. 9, and also due to the acoustic losses introduced by the Teflon insulating film and the epoxy layers. Our best estimation of the resonance frequency values are reported in Table 3 and are rather good if compared with those simulated with the three-port model. The bandwidth is instead difficult to

Table 3
Estimation of the IDT resonance frequency values

Parameter	Simulated data	Measured data
IDT electrical input impedance Z_{IN}		
First resonance frequency f_{R1} (kHz)	313	331
Second resonance frequency f_{R2} (kHz)	630	617
$ Z_{IN} @f_{R1}$ (Ω)	3000	3245
$ Z_{IN} @f_{R2}$ (Ω)	1641	1884

estimate for the uncertainty of the measured impedance magnitude.

For testing the Lamb waves propagation we excited the Tx-IDT with sine wave burst and a differential linear power amplifier with peak to peak amplitude of $V^+ = -V^- = 33$ V. (or 66 V_{pp} sine wave burst). The Rx-IDT is connected to a dedicated low noise instrumentation amplifier with—3dB bandwidth 1 MHz and 56 dB voltage gain.

The operating frequency f_0 and number of cycles have been tuned in order to have the best compromise between received signal amplitude and modes (k_1 and k_2) separation; considering the distance $D = 437$ mm between the embed-

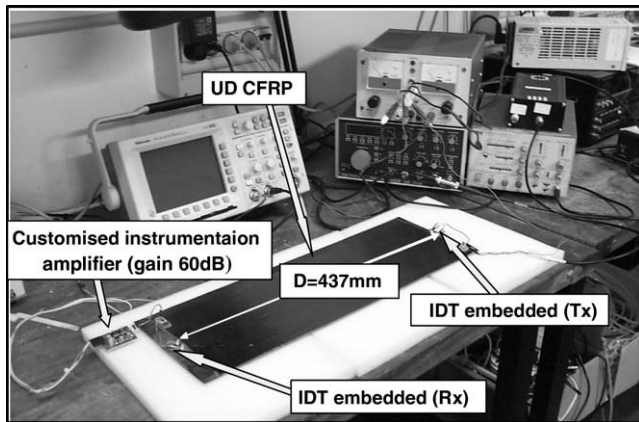


Fig. 8. Experimental set-up used to validate the design process.

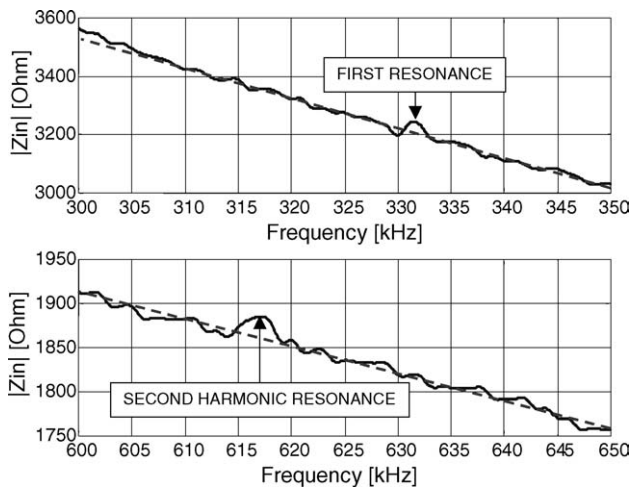


Fig. 9. Measured input impedance of the embedded interdigital transducer.

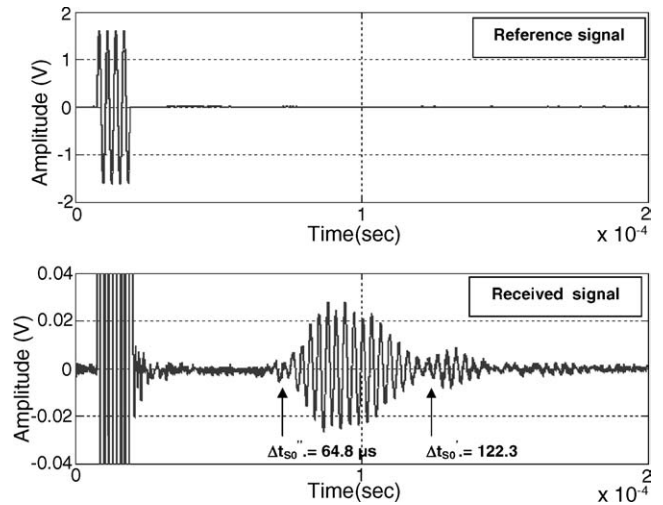


Fig. 10. Burst of four sinusoidal cycles at $f_0 = 350$ kHz used as reference signal (top) and received signal on the Rx-IDT (bottom). The predicted values of time of flight for the two propagation modes are indicated as $\Delta t_{SO}'$ and $\Delta t_{SO}''$.

ded IDT transmitter and receiver, was chosen $f_0 = 350$ kHz and a four cycles burst, as shown at the top of Fig. 10. For better understanding the modes propagation, the spectrum magnitude of this excitation signal has been added at the bottom of the viewgraph of Fig. 2A, with axis frequency multiplied by a factor $d = 3$ mm. At the bottom of Fig. 10 is shown the acquired signal averaged 32 times, composed by two wavelets: a “fast” one with higher amplitude (about 30 mVpp) followed by a second one with a smaller amplitude of about 18 mVpp. Assuming valid the estimated phase velocities reported in Table 1 for the two symmetrical modes at k_1 and k_2 , we have evaluated the expected time of flight for these two modes: $\Delta t_{SO}' = D/V_{SO}' = 122.3 \mu s$ and $\Delta t_{SO}'' = D/V_{SO}'' = 64.8 \mu s$. The time of flight reported for the two wavelets in Fig. 10 are in agreement with the expected phase velocity considering the approximation of the estimation of the elastic constant, the accuracy of the dispersion curves and the effect of the thin layer of epoxy (about 0.1 mm thickness) for bonding the two unidirectional carbon fiber composite plates.

In this viewgraph appears also an initial saturated signal generated by the electrical cross-coupling between the IDT due to the conductive plate of carbon fibres. Moreover, the time domain signal spreading occurred in this experiment is mainly due to the dispersive behavior of the propagating modes as already shown in Fig. 2A and the type of signal excitation used without any windowing function. This effect has been recently analyzed by Wilcox [20] and some techniques devoted to compensate for this have been presented.

The same pair of IDTs were also tested at lower operating frequencies to demonstrate the versatility and the efficiency of this transducer type to excite guided modes at lower $f \times d$ values. In Fig. 11B and C are illustrated the responses obtained with a sinewave burst excitation at 140 and 90 kHz,

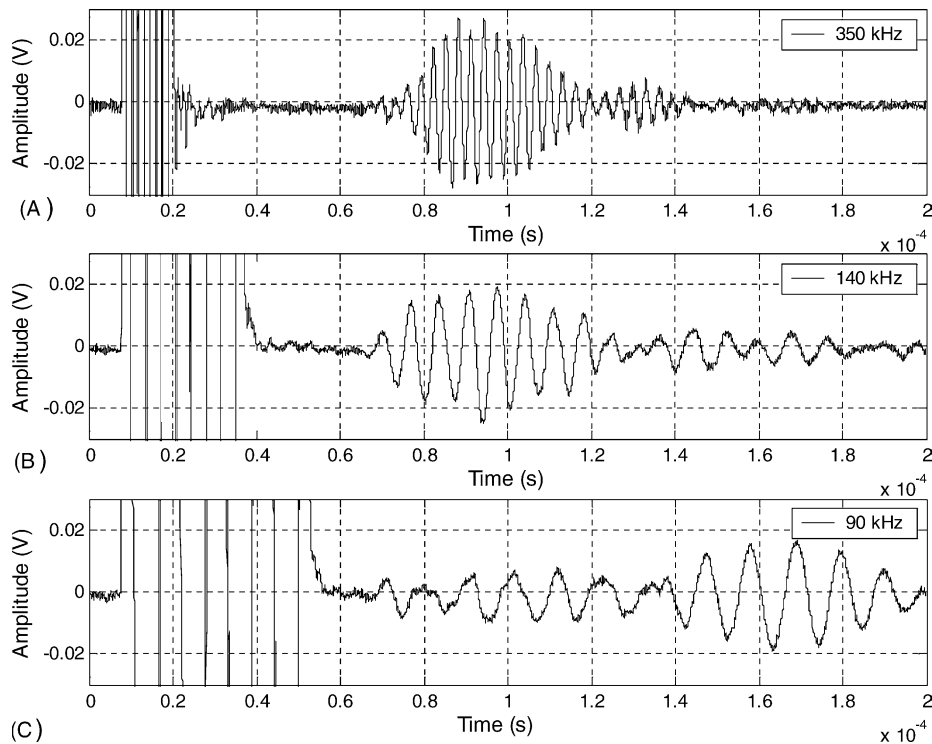


Fig. 11. Three received signals with a 4 sine wave cycle excitation at different frequency (A) 350 kHz, (B) 140 kHz, (C) 90 kHz.

respectively and compared with the response at 350 kHz (see Fig. 11A). We can observe in Fig. 11B that the amplitude of the received S_0 mode is comparable to that at 350 kHz, while in Fig. 11C an A_0 mode at lower phase velocity (starting at about 140 μ s) is generated with amplitude slightly diminished respect to the reference signal in Fig. 11A.

6. Conclusions

In this paper we demonstrated an efficient use of a pair of PVDF interdigital transducers designed for a wavelength 8 mm, embedded in a CFRP unidirectional composite laminate. A symmetrical S_0 mode guided wave has been propagated into a 3 mm thick composite at a Tx–Rx distance of about 0.5 m with a thin (100 μ m thickness) piezopolymer IDT with phase velocity close to simulated one.

The measurements of the guided modes agree well with the predicted modes obtained by simulations in terms of phase velocity. A simple model for evaluating the electrical impedance and the acoustic response of the IDT was developed and compared with experimental results. An electrical impedance magnitude around 3 k Ω was found at the operating mode 330 kHz \times 3 mm. A good efficiency was demonstrated with a 33 V differential sinewave burst excitation, covering a distance of 0.5 m with high S/N ratio.

However, the optimization of the transducer efficiency coupled to a specific composite laminate can be tackled with the delta V/V design method reported in [7]. From preliminary simulations [10] seems that a degree of optimization is

possible by changing the electrodes layout and will be investigated in a future research work.

In conclusion this work opens a perspective of piezopolymer IDTs manufactured with a low-cost and flexible design process to be used in NDT monitoring systems for large structures with sensors networks. The transducers embedding process during the composite manufacturing has not been demonstrated yet but is a clear objective for designing “smart composite materials” with auto-diagnostic capabilities.

References

- [1] J.L. Rose, Guided wave nuances for ultrasonic nondestructive evaluation, *IEEE Trans. Ultrason. Ferroelectr. Freq. Control* UFFC-47 (2000) 575–583.
- [2] B.A. Auld, *Acoustic Fields and Waves in Solids*, R.E. Kreiger Publishing Company, Malabar, FL, 1990.
- [3] ESA-ESTEC/Contract n. 16938/02/NL/MV Piezopolymer transducers for acoustic guided waves detection: application to non-destructive testing of composite laminates, University of Florence-Alenia Spazio/Laben.
- [4] A. Gachan, P. Reynolds, G. Hayward, R. Monkhouse, P. Cawley, Piezoelectric materials for application in low profile interdigital transducer designs, in: *Proceedings of the IEEE Symposium on Ultrasonics*, vol. 2, 1997, pp. 1025–1028.
- [5] R.H. Thomas, J.L. Rose, Flexible PVDF comb transducers for excitation of axisymmetric guided waves in pipe, *Sens. Actuators A: Phys.* 100 (2002) 18–23.
- [6] R.S.C. Monkhouse, P.D. Wilcox, P. Cawley, Flexible interdigital PVDF transducers for the generation of Lamb waves in structures, *Ultrasonics* 35 (1997) 489–498.

- [7] G.S. Kino, *Acoustic Waves—Devices, Imaging, and Analog Signal Processing*, Prentice-Hall, Englewood Cliffs New Jersey, 1987 (processing series, Chapter 2).
- [8] P.D. Wilcox, P. Cawley, M.J.S. Lowe, Acoustic fields from PVDF interdigital transducers, *IEEE Proc. Sci. Meas. Technol. SMT-145* (1998) 250–259.
- [9] N. Guo, P. Cawley, The interaction of Lamb waves with delaminations in composite laminates, *Acous. Soc. Am., ASA* (1993) 381–397.
- [10] Private communication from Prof. Pierre Khuri-Yakub, Ginzton Laboratory, Stanford University, July 2004.
- [11] G.G. Yaralioglu, F.L. Degertekin, K.B. Crozier, C.F. Quate, Contact stiffness of layered materials for ultrasonic atomic force microscopy, *J. Appl. Phys.* 87 (10) (2000) 7491–7496.
- [12] M. Veidt, T. Liu, S. Kitipornchai, Modelling of Lamb waves in composite laminated plates excited by interdigital transducers, *NDT&E Int.* 35 (2000) 437–447.
- [13] A. Gachagan, P. Reynolds, G. Hayward, A. McNab, Construction and evaluation of a new generation of flexible ultrasonic transducers, in: *Proceedings of the IEEE International Symposium on Ultrasonics*, San Antonio, USA, November 3–6 1996, pp. 853–856.
- [14] *Micromachining in Optoelectronics World, Supplement of Laser Focus World*, June, 2001, pp. 181–224.
- [15] L. Capineri, L. Masotti, M. Mazzoni, G. Masotti, Microfabrication Technology for polymer pyroelectric sensor arrays, *MME'03 Meet*, Delft, The Netherlands, 2–4 November 2003, pp. 147–150.
- [16] L. Capineri, A. Gallai, L. Masotti, M. Materassi, Piezopolymer transducer for acoustic guided waves detection: application to non-destructive testing of composite laminates, in: *Ultrasonics Symposium, Proceedings 2002 IEEE*, vol. 1, 8–11 October 2002, pp. 857–860.
- [17] L.F. Brown, Design Considerations for piezoelectric polymer ultrasound transducers, *IEEE Trans. Ultrason. Ferroelectr. Freq. Control* UFFC-47 (2000) 1377–1396.
- [18] J. Jin, S.T. Quek, Q. Wang, Design of interdigital transducers for crack detection in plates, *Ultrasonics*, in press.
- [19] P.D. Wilcox, R.S.C. Monkhouse, P. Cawley, M.J.S. Lowe, B.A. Auld, Development of a computer model for an ultrasonic polymer film transducer system, *NDT&E Int.* 31 (1998) 51–64.
- [20] P.D. Wilcox, A rapid signal processing technique to remove the effect of dispersion from guided wave signals, *IEEE Trans. Ultrason. Ferroelectr. Freq. Control* UFFC-50 (2003) 419–427.

Biographies

Andrea Bulletti received the Electronic Engineering Laurea degree from the University of Florence, Italy, in 2002. From June 2003 to December 2004 he has been working as contract researcher at Department of Electronics and Telecommunications of the University of Florence. His research interests concern non-destructive testing methods for high-voltage dielectric materials and composite materials.

Filippo Bellan, he earned the Laurea degree in Electronic Engineering in 2004 with a thesis on guided waves ultrasonic transducers. He is now employed with the company EL.M. Spa (Prato, Italy).

Francesco Guasti, he earned the Laurea degree in chemistry on 1990 at the University of Florence. Since 1991 he works with Alenia Spazio

Laben Division and his current research activity is devoted to advanced composite materials, metallurgical processes, organic and inorganic synthesis processes.

Lorenzo Capineri, since 2003 is associated professor in Electronics and now is working at Department of Electronics and Telecommunications of the University of Florence, Italy. His current research activities are in design of ultrasonic and pyroelectric sensors, signal and image processing for ultrasonic and ground penetrating radar systems.

Leonardo Masotti, Leonardo Masotti was born in Faenza, Italy, in 1939. He received the Laurea Degree in electronic engineering at the Faculty of Engineering in Bologna, Italy, in 1963 and the Italian national Libera Docenza degree in applied electronics in 1970. His present position is full professor of electronics and research director of the Ultrasound and Non-Destructive Testing Laboratory at the Department of Electronics and Telecommunications of the University of Florence, Italy. He has been a member of the Scientific Committee of the Istituto di Elaborazione dell'Informazione of CNR in Pisa since 1983 and of the Scientific Committee of Istituto di Fisiologia Clinica of CNR in Pisa since 1989. He has been President of the Consorzio Centro di Eccellenza Optronica (CEO) since 1992. He also takes part in the Technical Direction Committee of the High Tech Network for the Tuscany Region.

Edgardo Rosi received the electronic engineering degree from the University of Florence, Italy, in 1976. Since 1987 he works with Alenia Spazio Laben Division and his current research activity is devoted to advanced composite materials, new processes for composite production and space technology.

Goksen G. Yaralioglu was born in Akhisar, Turkey on 13 May 1970. He received his BS, MS and PhD degrees from Bilkent University, Turkey, in 1992, 1994, and 1999, respectively, all in electrical engineering. He is now working as an engineering research associate in E.L. Ginzton Laboratory, Stanford University. His current research interests include design, modeling and applications of micromachined ultrasonic transducers, and atomic force microscopy at ultrasonic frequencies.

F. Levent Degertekin received his PhD degree from Stanford University in electrical engineering. He is currently an assistant professor at the mechanical engineering department of Georgia Institute of Technology. His research interests are in the field of micromachined sensors and actuators and their applications. One of his research topics is capacitive micromachined ultrasonic transducers (cMUTs). The work on cMUTs for medical ultrasound imaging includes transducer optimization, cross talk reduction, and electronics integration in one- and two-dimensional medical imaging arrays. Design and fabrication of cMUT-based Lamb wave and surface acoustic wave devices as sensors and electronic filters is another topic of his research in this area.

B.T. Khuri-Yakub was born in Beirut, Lebanon. He received the PhD degree in 1975 from Stanford University, in electrical engineering. He is currently a Professor of Electrical Engineering (Research) at Stanford University. His research interests include in situ acoustic sensors (temperature, film thickness, resist cure, etc.) for monitoring and control of integrated circuits manufacturing processes, micromachining silicon to make acoustic materials and devices such as airborne and water immersion ultrasonic transducers and arrays, and fluid ejectors, and in the field of ultrasonic non-destructive evaluation and acoustic imaging and microscopy. His group at Stanford University also focuses on the development of capacitive micromachined ultrasonic transducers (cMUTs) for medical imaging.